J Mater Sci (2009) 44:5829–5835
DOI 10.1007/s10853-009-3821-0

Formation of dendritic precipitates in the beta phase of Cu-based alloys

M. L. Castro · O. Fornaro

Received: 11 May 2009 / Accepted: 18 August 2009 / Published online: 2 September 2009

Abstract The isothermal treatment of the β phase in some Cu-based alloys produces its decomposition by an earlier precipitation of γ phase. During their growth, by means of a diffusion-controlled process, the precipitates show evidences of morphological changes. In the first stages and for a Cu–Zn–Al alloy, the morphology is spherical and cuboidal, but develops more complex shapes such as dendrites, owing to composition fields, interphase overlapping, crystallography characteristics, and relative orientation. In this work, a dendritic γ precipitate characterization is done and morphological theoretical predictions are applied, for Cu–Zn–Al and Cu–Al–Be alloys.

Introduction

Cu-based alloys are Hume-Rothery materials for which the stability of different phases, at different compositions and temperatures depends, mainly, on the average number of conduction electrons per atom, or electron to atom ratio (e/a). At e/a $\approx$ 1.5 and high temperature, these alloys display a bcc structure (β phase). In general, at lower temperatures the β phase is not stable and a decomposition process to stable phases takes place. However, the β phase can be retained below its stability limit by means of suitable thermal treatment, owing to that increasing the cooling rate from high temperature the equilibrium phases can be partially or totally suppressed.

M. L. Castro (✉) · O. Fornaro
Investigador CONICET: Comisión Nacional de Investigaciones Científicas, Instituto de Física de Materiales Tandil (IFIMAT-CICPBA-MT), Universidad Nacional del Centro de la Provincia de Buenos Aires, Pinto 399, Tandil B7000GHG, Argentina
e-mail: mlcastro@exa.unicen.edu.ar

During the cooling, the metastable β phase can suffer one or two ordering transitions, to a B2, CsCl superlattice, and/or DO_3 or $L2_1$ (Cu_2MnAl) superlattices. Besides, depending on composition, these alloys are able to undergo a diffusionless, first order, structural transition known as martensitic transformation responsible for the shape-memory properties exhibited by this material.

For the Cu–Zn–Al system the stability range of the β phase decreases with decreasing temperature, and centers around an electron concentration of $\approx$1.48. This metastable phase can undergo a diffusive decomposition to the equilibrium phases, generally α and γ, during cooling [1–5] or by isothermal treatments at moderate temperatures, between 473 and 773 K [6–8]. This fact leads to a degradation of the shape-memory capacity and a change in martensitic transformation temperatures [9–11].

The Cu–Al–Be alloy is, as Cu–Al–Ni, an alloy derived from the Cu–Al one. For the Cu–Al the stable β-phase domain exhibits an eutectoidal point around 24 at.% Al and 823 K. Below the range of stability of the β phase, the equilibrium phases are the α (fcc structure) and γ_2 (Cu_9Al_4 structure) phases, with low and high Al content, respectively. At lower temperature, it exhibits a martensite transformation from the DO_3 to an 18R close-packed structure [5].

The morphology of the precipitated phases depends on many factors such as composition, crystallography, thermal treatment characteristics: temperature, time, cooling rate. The morphology of the γ phase is basically cuboidal but in some cases the formation of solid-state dendrites is observed. The formation of solid-state dendrites has received little attention in the past, in spite of being a rare phenomenon reported in few systems. Shewmon noted that the dendritic morphologies are rarely observed in the solid–solid systems [5, 12, 13]. Earlier it was reported that the γ

Table 1 Nominal composition of the alloys (at.%)

	Cu	Al	Zn	Be
CAZ	68.33	16.33	15.34	
CAB	73.73	22.72		3.55

precipitates were formed in the dendritic shape when Cu–Zn β-phase alloys were cooled from high temperatures. Doherty discussed various factors that appear to explain the shape instabilities in solid-state reactions [14].

Husain et al. [15] observed γ precipitates formed in a dendritic shape in the Cu–Al β-phase alloys. They analyzed special characteristics of two alloy systems: Cu–Al and Cu–Zn, in which such morphology has been observed in the solid-state precipitation; and predicted other systems in which such morphologies should occur.

In this work, we present observations of γ precipitation in the β phase of a Cu–Zn–Al and a Cu–Al–Be alloy. We analyzed the dendritic morphology observed in terms of recent theories of dendritic growth.

Experimental

Single crystals of nominal composition Cu–15.34 Zn–16.33 Al and Cu–22.72 Al–3.55 Be (at.%) were used (Table 1). Disc-shaped samples, having a diameter of about 6 mm and a thickness of 1.5 mm, were cut using a low-speed diamond saw. The aging treatments were carried out in a resistance-heated furnace, with electronic temperature control maintaining a constant temperature $\sim$1 K. The specimens were heated to 1093 K, within the β-phase field, for about 1 h, followed by an air cooling to room temperature (RT) before isothermal aging at temperatures between 473 and 773 K.

Optical micrographic observations (OM) and electron microscopy (Hitachi S530 SEM, Hitachi H600 a 100 kV TEM and JEOL 2011 HRTEM) were made after a careful electropolishing and etching of the specimens with a saturated solution of CrO_3 in phosphoric acid and then, in a $FeCl_3$–HCl–H_2O solution. For TEM/HRTEM the specimens were double-jet electropolished at RT in an electrolyte containing 47% water, 24% orthophosphoric acid, 24% ethanol and 5% propanol, and urea, at 8 V.

Results and discussion

Microstructural observations

In general, isothermal treatments at moderate temperatures, between 473 and 773 K, in Cu-based SM alloys with an electron atom ratio e/a near the eutectoid one (1.50) produce the β-phase decomposition into the equilibrium α and γ phases [6–8, 16, 17]. The original structure of the alloys after air cooling from 1093 K and prior to the aging treatment is that of the ordered β phase ($L2_1$ for the Cu–Zn–Al alloy and DO_3 for de Cu–Al–Be one). In the studied cases, the first particles observed were precipitates of γ phase, followed by precipitates of α phase. Both alloys are situated near the eutectoid position, then after prolonged isothermal aging a final eutectoid structure is observed. The morphological evolution of the precipitates of γ and α phases until they reach this final structure depends on the aging temperatures.

As can be seen in Fig. 1a–d, for the Cu–Zn–Al alloy, the dendritic shape of the γ precipitates is observed for different temperatures during the treatments. In the first stages the precipitates have a circular/polyhedral shape (Fig. 2a), increasing the thermal treatment time, they take a cuboidal shape and develop dendritic characteristics but conserving the cuboidal aspect, for temperatures lower than 573. For higher ones, the dendritic morphology develops earlier in the thermal process, and the arms are more marked. Likewise, it is observed that the principal dendrites and secondary arms are oriented in preferential directions. For temperature near and higher 770 K, the γ phase particles showed a polyhedrical morphology with a tendency to spherical shape (Fig. 2b).

In the case of the Cu–Al–Be alloy, the Fig. 3 shows γ precipitates for different times in the temperature range 623–723 K. They present different shapes between globular–cuboidal and regular–irregular; but for temperatures higher than 773 K, the γ precipitates showed a dendritic shape, with main arms in perpendicular directions (Fig. 4).

The particle shape in the solid–solid precipitation could be influenced by various factors such as the rate of diffusion, kinetics of the interfacial reaction, interfacial energy, anisotropy of the parent phase, and the crystallographic features of the precipitates and the parent phase. According to Shewmon [12] if solute diffusion alone determines the growth rate of a precipitate growing from the supersaturated parent phase, the precipitate shape will have characteristics of dendrites found in solidification. However, this shape is rarely observed in the solid-state precipitation reactions because other stabilizing factors keep the interface smooth. The kinetics of addition of atoms to the growing interface plays an important role in determining the morphology of the growing phase. The dendritic morphology is favored when this kinetics is fast, and this happens when the structures of the phases involved are similar, so the crystallographic similarities between the precipitate and the parent phase would be favorable. This includes similarities in the crystal structure, low mismatch in the lattice parameters, and favorable orientation

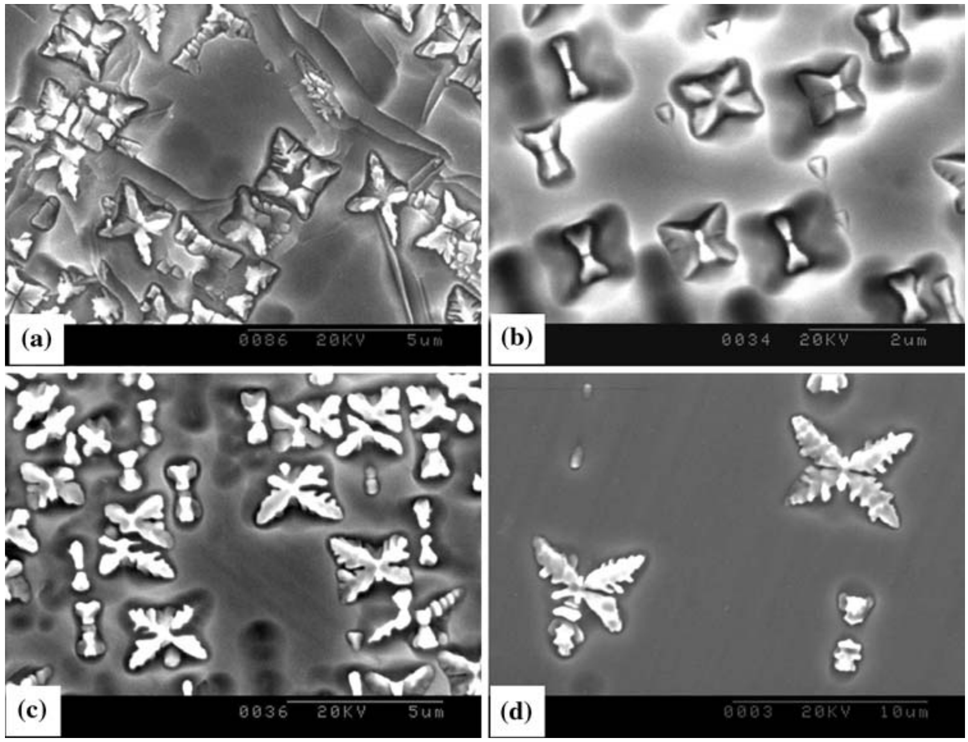

Fig. 1 Scanning electron micrograph for CZA alloy, with the following isothermal treatment: **a** 380 h at 473 K, **b** 7 h at 520 K, **c** 1320 min at 600 K, **d** 10 min at 650 K

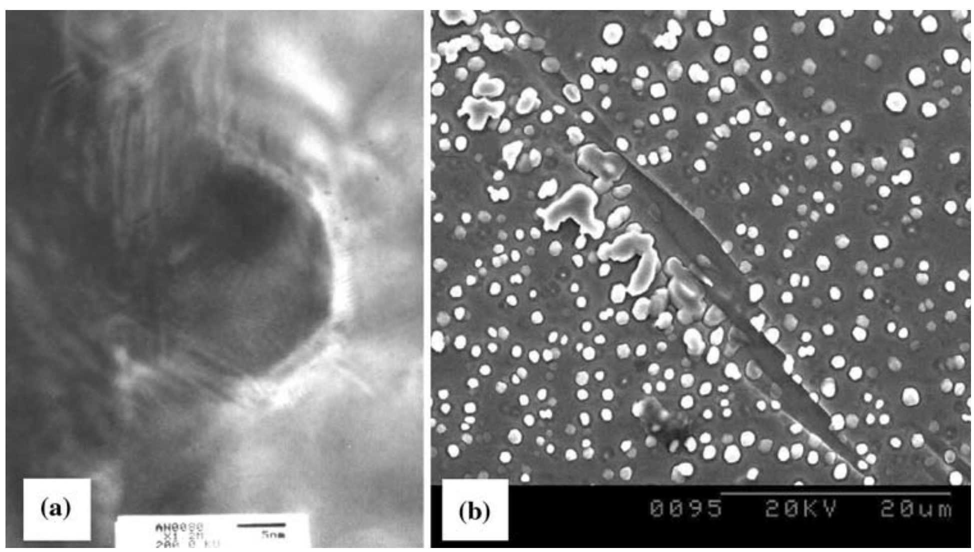

Fig. 2 Gamma precipitates in CZA alloy: **a** HRTEM micrograph formed during aging at 600 K; **b** SEM micrograph after 5-h treatment at 770 K

relationships. So, the crystallographic similarities between the parent phase and the precipitate are a dominant factor giving rise to the dendritic morphology of the precipitates [15].

Pons and Portier [1, 2] had observed a perfect continuity of the atomic planes in the β matrix and the γ precipitates in CZA alloys by HRTEM images, similar to the one in Fig. 2a. This is a consequence of the cube–cube type orientation relationships and the very small misfit between both structures (near 0.7%). The precipitates are well-allocated inside the parent phase, i.e., the elastic and interfacial energies are relatively low. The coherency of the precipitates is lost when they reach sizes of about 50 nm, and misfit dislocations form at the interfaces [1].

In the present case, the high-temperature β phase has a bcc structure. The γ phases have a complex bcc structure and are usually ordered. The precise form of order varies with the ratio of solvent to solute atoms between $D8_1$ and $D8_3$ type [18]. In the Cu–Al systems it has $D8_3$ structure while in the Cu–Zn one it is $D8_2$. Both $D8_2$ and $D8_3$ are

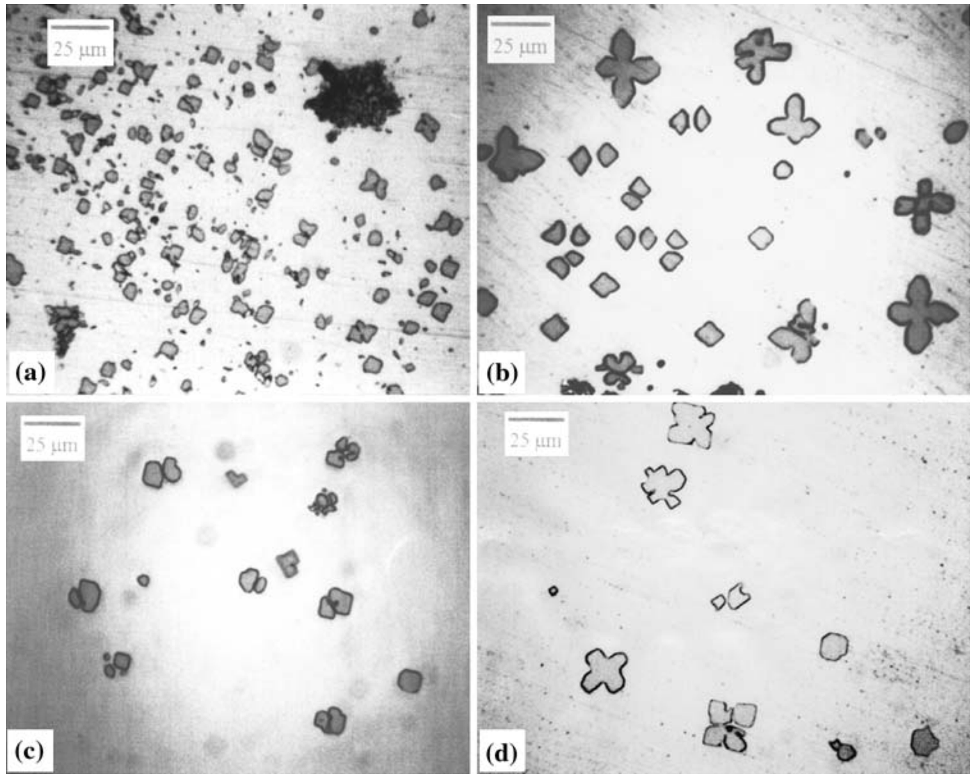

Fig. 3 Optical micrograph for CAB alloy with the following isothermal treatment: **a** 290 h at 620 K, **b** 124 h at 663 K, **c** 19 h at 740 K, **e** 5 h at 780 K

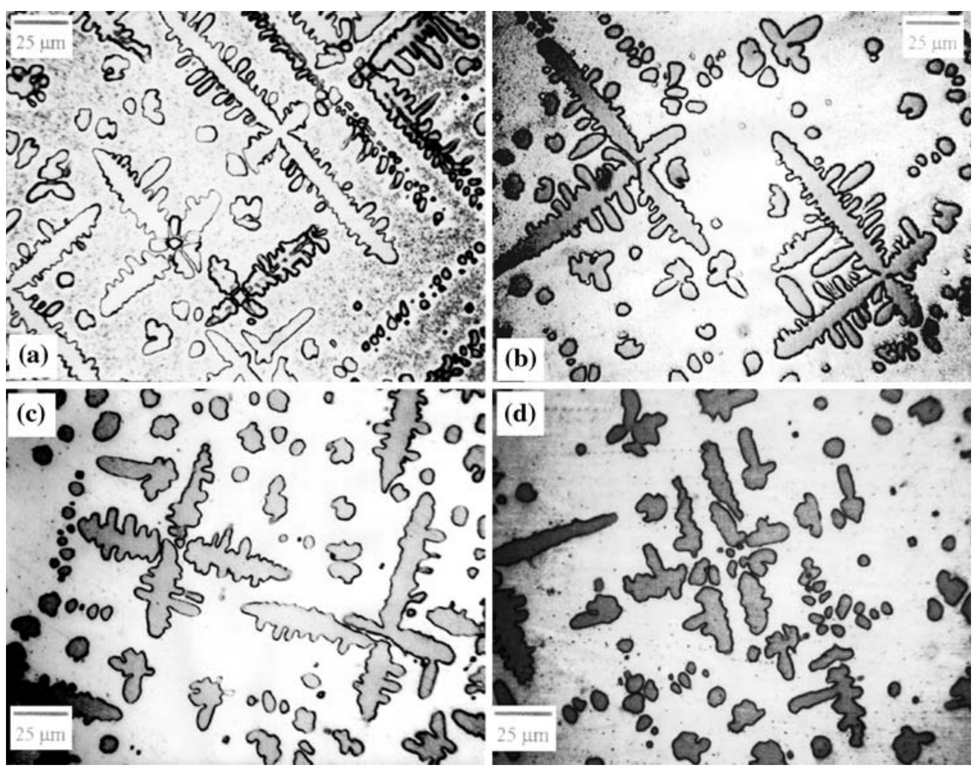

Fig. 4 Optical micrograph for CAB alloy with isothermal treatment at 790 K for: **a** 2 h, **b** 5 h, **c** 21 h, **d** 42 h

superlattices containing 52 atoms per unit cell. These lattices are basically formed by $3 \times 3 \times 3$ bcc unit cells. The lattice parameters are also closely related; the lattice parameter of the precipitate is almost 3 times the lattice parameter of the parent phase. The β and γ lattices are almost identical; there exists a three-dimensional lattice matching in these alloy systems [19, 20]. Hence during the precipitation process, the diffusing atoms do not face any difficulty in attaching themselves to the growing interface, giving form to a dendritic shape. Furthermore, fast bulk diffusion is necessary for the dendritic morphology occurs; but diffusion is very rapid in β phases in both Cu–Al and Cu–Zn systems.

In the present Cu–Zn–Al alloy, with intermediate composition between Cu–Zn and Cu–Al, dendritic precipitates are observed at low temperatures where the β phase has $L2_1$ order. If we compare this behavior with the one observed by Hussains et al. [15] for Cu–Sn alloys, we will infer that the γ precipitates in our alloy have $D8_{1-3}$ structure.

As could be seen in Figs. 1, 2, 3, and 4, the dendritic precipitate arms grow in well-defined directions. It was possible to determine the angle between primary arms (θ) in the range of 67°–72°; while these arms are perpendicular in the case of the Cu–Al–Be alloy. The secondary arms, when observed, are in direction close parallel to the others primary ones (Fig. 5). The measured relationship between the secondary arms distance (λ_2) and the curvature ratio of the tip (ρ) is

$$\rho = 0.5\lambda_2;$$

which is a similar condition to the one observed during crystal growth in undercooled liquids [21, 22]. Typical values obtained in precipitates like the one showed in Fig. 5 are listed in Table 2.

Simulations

Taking into account that dendritic growth of the precipitates is a consequence of an anisotropic interfacial energy, and of the characteristic orientation of their primary and secondary arms, it is possible to consider that the perturbations belong such orientations are a consequence of crystallographic orientation. Following the treatment proposed originally by Mullins and Sekerka [23, 24] we induce periodic perturbations over an originally spherical surface, in such a way that, at whatever time, the interface is described by

$$r = p(\theta, \phi, t) = r_0 + \delta(t) Y_{lm}(\theta, \phi) \quad (1)$$

where r_0 is the initial radius of the precipitate, $\delta(t)$ and $Y_{lm}(\theta,\varphi)$ are, respectively, the temporal and the spatial contribution to the surface perturbation. The full solution

Table 2 Morphological parameters of the dendritic precipitates (μm)

	Primary arm length	λ_2	ρ
CAZ	1.8	0.32	0.15
CAB	87	5	2.33

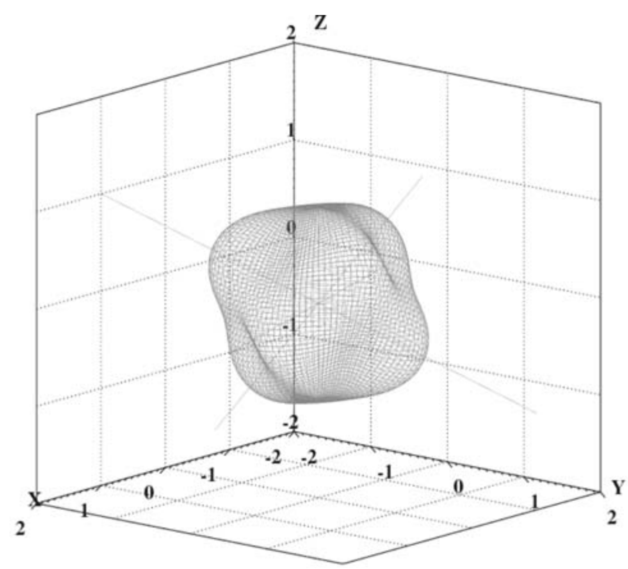

Fig. 6 First stages schematic draw of periodic perturbations over an initially spherical precipitate

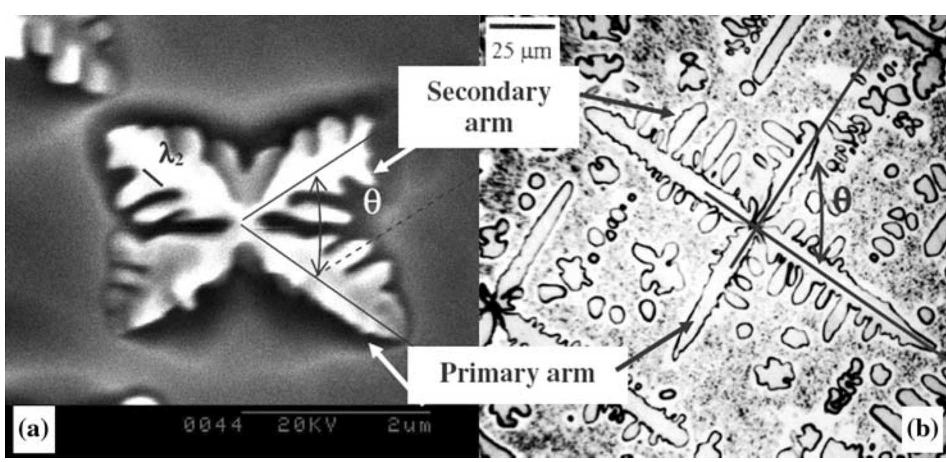

Fig. 5 Dendritic precipitation observed after **a**1320 s at 600 K in a CZA alloy (SEM); **b** 2 h at 790 K in the CAB alloy (OM)

includes the solution of temporal term for each possible harmonic. We assume that this solution exists, is real and positive, and focus in the spatial term, particularly to the spherical harmonics of the type Y_{4n}, which describes cubic symmetries. In these cases, the precipitates, which originally are close to a spherical geometry, assume a cubic morphology (Fig. 6), and next, promote the apparition of the small primary arms, in the same way as is experimentally observed. This distortion could follow a characteristic direction if the perturbation continues growing, but the equations shown before only describe the start of primary arms for small distortions. Under this model, given by a symmetry of Y_{43}, an sphere can develop six arms. In the Fig. 7 it is possible to observe four of them; the other two are located on top and below the figure plane. Please note that these arms are not normal to the figure plane. By other side, as can be seen in Fig. 8, the Y_{42} family perturbation let us to observe the normal primary arms. Figure 9 suggests the time evolution of an initially spherical precipitate, being disturbed by a wave function Y_{42}.

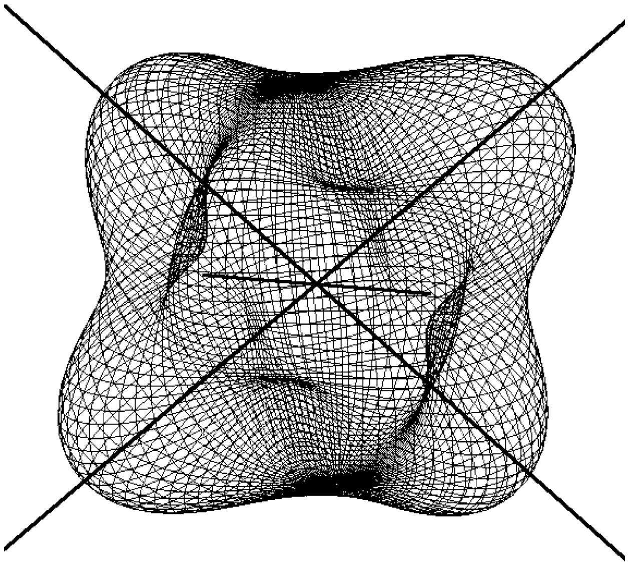

Fig. 7 Schematic draw of an initially spherical surface distorted with Y_{43} symmetry

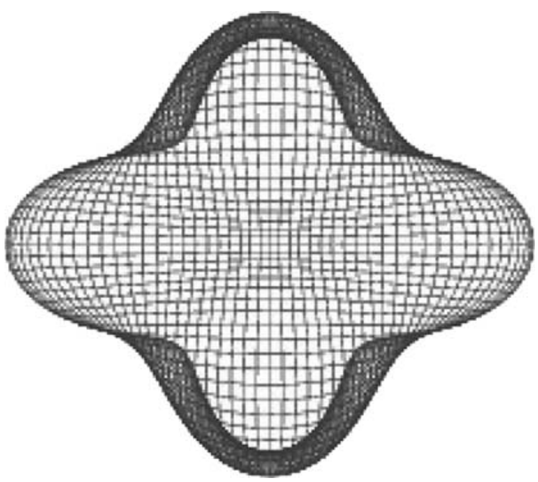

Fig. 8 Schematic draw of an initially spherical surface distorted with Y_{42} symmetry

In all the cases described, the model qualitatively schematizes the directions where the amplitude $p(t)$ has a greater variation, under the supposition that it was originally spherical and unstable.

Conclusions

By isothermal treatments at moderate temperatures, between 473 and 773 K, γ precipitation in the β phase of a Cu–Zn–Al and a Cu–Al–Be is observed. These precipitates developed a dendritic morphology with arms growing in well-defined directions and a relationship between the secondary arms distance and the curvature ratio of the tip similar to the one observed during crystal growth in undercooled liquids.

In the Cu–Al–Be alloy this morphology is observed for temperatures higher than 773 K, while for the Cu–Zn–Al one, the γ precipitates showed a dendritic shape at lower temperatures where the β phase has $L2_1$ order.

The application of a simple model consisted in inducing periodic perturbations over an originally spherical surface, describes quite well the experimental morphologies observed.

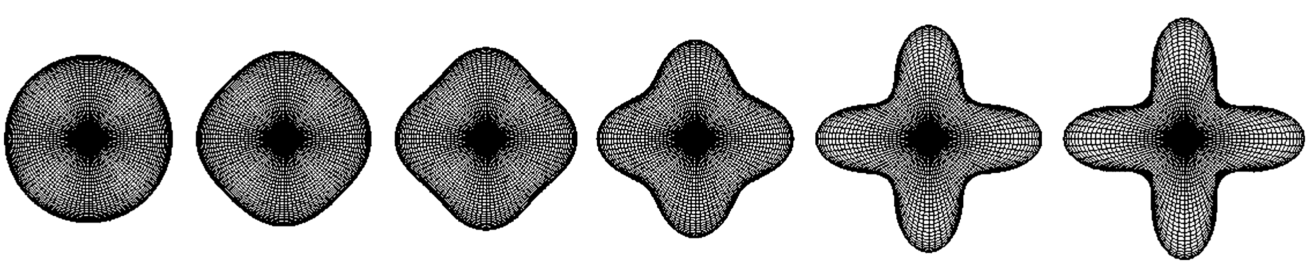

Fig. 9 Suggested evolution of an initially spherical precipitate disturbed by a wave function Y_{42}

Acknowledgements This work was partially supported for the Ministerio de Educación y Cultura of Spain by a research grant in the Department de Física, Universitat de les Illes Balears; and by the ANPCyT and CONICET, CIC and the Secretaría de Ciencia, Arte y Tecnologia of the Universidad Nacional del Centro, Argentina.

References

1. Pons J, Portier R (1997) Acta Metall 45:2109
2. Pons J, Portier R (1995) J Phys IV C2:245
3. Lovey FC, Cesari E (1990) Mater Sci Eng A129:127
4. Zhang LC, Aindow M (2006) J Mater Sci 41:611. doi:10.1007/s10853-006-6477-z
5. Ochoa-Lara MT, Florez-Zuñiga H, Rios-Jara D (2006) J Mater Sci 41:5455. doi:10.1007/s10853-006-0295-1
6. Castro ML, Romero R (1998) Mater Sci Eng A255:1
7. Castro ML, Romero R (1999) Mater Sci Eng A273–275:578
8. Castro ML, Romero R (1999) Isothermal precipitation in a β Cu–Zn–Al SM alloy. In: Proceedings of the international conference on solid–solid phase transformation, The Japan Institute of Metals, vol 12, pp 221–224
9. Garcia J, Pons J, Cesari E (1996) Mat Res Bull 31:709
10. Auguet C, Cesari E, Rapacioli R, Mañosa Ll (1989) Scr Metall 23:579
11. Lovey FC, Cesari E, Auguet C, Mañosa Ll, Rapacioli R (1990) Mater Sci Forum 56–58:493
12. Shewmon PG (1965) Trans TMS-AIME 233:736
13. Watanabe D, Watanabe C, Monzen R (2008) J Mater Sci 43:3946. doi:10.1007/s10853-007-2373-4
14. Doherty RD (1996) In: Cahn R, Haasen P (eds) Physical metallurgy, vol 2, 4th edn. North-Holland, Amsterdam, p 1421
15. Husain SW et al (1999) Metall Mater Trans 30A:1529
16. Castro ML, Romero R (2000) Scr Mater 42:157
17. Castro L, Romero R (2000) Mater Sci Eng A287:66
18. Massalski T, King H (1963) Prog Mater Sci 10:50
19. Woo S et al (1944) Trans AIME 156:100
20. Malcolm JA, Purdy GR (1967) Trans AIME 239:1391
21. Langer JS (1980) Rev Mod Phys 52(1):1
22. Kurz W, Fisher JD (1989) Fundamentals of solidification. Trans Tech Publications, USA
23. Mullins WW, Sekerka RF (1963) J Appl Phys 34:323
24. Fornaro O, Palacio H (2006) Scr Mater 54:2149